A position estimation method for active magnetic bearings based on the star point voltage

Jonah VENNEMANN*, Niklas KÖNIG*, Rudolf GERLICH* and Matthias NIENHAUS*
* Laboratory of Actuation Technology, Saarland University
Campus E2 9, 66123 Saarbrücken, Germany
E-mail: vennemann@lat.uni-saarland.de

Abstract
Self-sensing position estimation methods for active magnetic bearings allow for the reduction of system cost and complexity. Many known methods rely on current measurements or their derivatives to estimate the rotor position. However, measuring a voltage often results in a better signal-to-noise ratio compared to current measurements. Despite that, star-connected active magnetic bearings and the related star point voltage, are rarely addressed in research. This is notable, as the star point voltage provides valuable information for self-sensing in other types of electric machines. This research aims to utilise the star point voltage of an active magnetic bearing to estimate the rotor position. The outlined study shows an analytical derivation of the star point voltage for a four-phase active magnetic bearing followed by a description of a differential measurement procedure for the star point voltage. It is demonstrated that the resulting measurements only depend on the coils inductance and the known DC supply voltage. To extract the position information from the obtained signal, the plant is characterised at standstill. The resulting measurements were used for polynomial fits, implemented on the microcontroller. Finally, the proposed method is experimentally validated inside the control loop. Different experiments show mean absolute estimation errors ranging from 0,8μm to 10μm.

Keywords : self-sensing, active magnetic bearing, AMB, star point, sensorless

1. Introduction

Self-sensing position estimation for active magnetic bearings (AMB) has been an active research topic for many years. Throughout these years, different techniques emerged that allowed a reduction of costs and contributed to condition monitoring and thus, the safety of AMBs (Maslen and Schweitzer, 2009). These techniques have various working principles. Among others, numerous self-sensing techniques rely on current measurements or their derivatives to estimate the inductance variation of the system and thus, the rotor position (Niemann and van Schoor, 2010; Nenning and Hutterer, 2014). However, the measurement of a current brings some challenges with it. For example, the signal-to-noise ratio (SNR) is often worse, compared to a voltage measurement. This can be particularly problematic if the derivative of the current is used. Considering other electric machines, like synchronous motors, exploiting the star point voltage led to robust and established methods with high SNR (Grasso, 2021; Schuhmacher, 2022). In contrast to the other electric machines, AMBs are not normally connected to the star point. Thus, the exploitation of the star point voltage and its interpretation has rarely been investigated (García et al., 2010). However, it is indeed possible to drive an AMB in a star configuration and observe a non-zero star point voltage (Brasse et al., 2023; Vennemann et al., 2023) carrying useful information. Measuring the star point voltage instead of a current promises a better SNR, also on AMB. This work aims to investigate the behaviour of the star-connected AMB and proposes a self-sensing technique based on differential measurements of the star point voltage. The presented method is based on a procedure called Direct Flux Control (DFC) which was developed for synchronous motors (Thiemann et al., 2011).

The rest of the paper is structured as follows: Section 2 describes the used circuitry and derives an expression for the star point voltage of the AMB along with a description of the proposed measurement and position extraction procedure. Section 3 shows the results of the experimental validation, followed by the discussion and future work in section 4.

2. Methodology

2.1. Mathematical description of the star point voltage

Figure 1 shows the electrical connection for the proposed position estimation technique. A two-stage inverter is used to drive the 4 phases of the AMB. In this diagram v_{DC} denotes the DC supply voltage, $v_{t,X}$ is the terminal voltage of the coils, v_X is the voltage across the coils, i_X is the coil current for $X \in \{A, B, C, D\}$, v_S is the star point voltage, Z is a measurement impedance between the star point and ground, v_{SA} is the voltage between the artificial star point and the star point. The drive and inverter are explained in detail by Brasse et al. (2023).

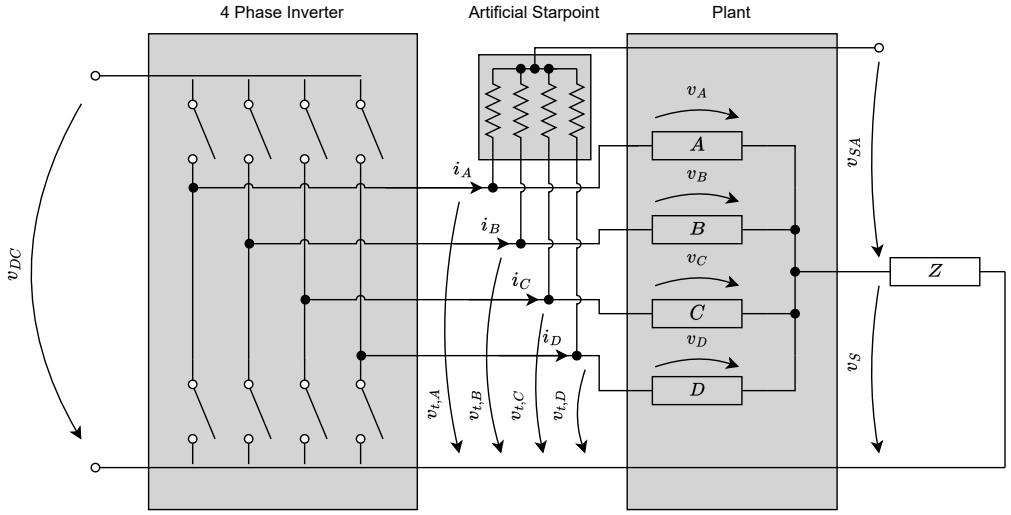

Fig. 1: Equivalent circuit diagram with inverter, star point and artificial star point of a star connected active magnetic bearing.

In order to derive an expression for the star point voltage, it is first necessary to describe the voltage in the single coils. The induced voltage in a single coil can be expressed with the help of Faradays law of induction

$$\epsilon_X = N \cdot A \cdot \frac{\mathrm{d}}{\mathrm{d}t} [B_X] . \tag{1}$$

where N is the number of windings per coil, A is the area of the air gap and B_X is the magnetic flux density in the air gap caused by the respective coil. Neglecting the influence of the iron core, Ampères circuital law provides an expression for the magnetic flux density in the air gap:

$$B_X = \frac{\mu_0 \cdot N \cdot i_X(t)}{2 s_X(t)} \tag{2}$$

where $s_X(t)$ is the size of the air gap and $i_X(t)$ is the current in the coil. For improved readability let $i_X(t) = i_X$ and $s_X(t) = s_X$ in the following. Inserting Eq. 1 into Eq. 2 and applying the quotient rule to the resulting term leads to:

$$\epsilon_X = \frac{N^2 \cdot A \cdot \mu_0}{2 s_X} \cdot \frac{\mathrm{d}i_X}{\mathrm{d}t} - \frac{N^2 \cdot A \cdot \mu_0 \cdot i_X}{2 s_X^2} \cdot \frac{\mathrm{d}s_X}{\mathrm{d}t} . \tag{3}$$

Introducing

$$L_X = \frac{N^2 \cdot A \cdot \mu_0}{2 s_X} \tag{4}$$

and adding the resistive voltage drop leads to the final expression for the voltage in a single coil:

$$v_X = R_X \cdot i_X + L_X \cdot \frac{\mathrm{d}i_X}{\mathrm{d}t} - L_X \cdot \frac{i_X}{s_X} \frac{\mathrm{d}s_X}{\mathrm{d}t} . \tag{5}$$

This equation can be expressed in matrix notation, to represent the proposed star connected, four-phase AMB:

$$\boldsymbol{v} = \boldsymbol{R} \cdot \boldsymbol{i} + \boldsymbol{L} \cdot \frac{d\boldsymbol{i}}{dt} - \boldsymbol{L} \cdot \frac{\boldsymbol{i}}{\boldsymbol{s}} \frac{d\boldsymbol{s}}{dt} \tag{6}$$

©2025 The Japan Society of Mechanical Engineers

with

$$\boldsymbol{v} = \begin{bmatrix} v_a \\ v_b \\ v_c \\ v_d \end{bmatrix}, \boldsymbol{R} = \begin{bmatrix} R & 0 & 0 & 0 \\ 0 & R & 0 & 0 \\ 0 & 0 & R & 0 \\ 0 & 0 & 0 & R \end{bmatrix}, \boldsymbol{L} = \begin{bmatrix} L_a & 0 & 0 & 0 \\ 0 & L_b & 0 & 0 \\ 0 & 0 & L_c & 0 \\ 0 & 0 & 0 & L_d \end{bmatrix}, \boldsymbol{i} = \begin{bmatrix} i_a \\ i_b \\ i_c \\ i_d \end{bmatrix}, \boldsymbol{s} = \begin{bmatrix} s_a \\ s_b \\ s_c \\ s_d \end{bmatrix}.$$

Here R denotes the resistance of a coil. It is assumed that the resistances of all coils are equal. It is further possible to express the voltage in the coil as the difference between the star point voltage and the terminal voltage $\boldsymbol{v}_t$ applied at the terminals of the inverter:

$$\boldsymbol{v} = \boldsymbol{v}_t - v_S \cdot \boldsymbol{T} \text{ with } \boldsymbol{T} = \begin{bmatrix} 1 \\ 1 \\ 1 \\ 1 \end{bmatrix}, \quad \boldsymbol{v}_t = \begin{bmatrix} v_{t,A} \\ v_{t,B} \\ v_{t,C} \\ v_{t,D} \end{bmatrix}. \tag{7}$$

Inserting Eq. 7 into Eq. 6 and isolating the current derivative yields:

$$v_S \boldsymbol{L}^{-1}\boldsymbol{T} = \boldsymbol{L}^{-1}v_t - \boldsymbol{L}^{-1} \cdot \boldsymbol{R} \cdot \boldsymbol{i} - \frac{d\boldsymbol{i}}{dt} + \frac{\boldsymbol{i}}{\boldsymbol{s}}\frac{d\boldsymbol{s}}{dt}. \tag{8}$$

If the current is measured with a high impedance Z or the star point is open, the sum of all currents i_X equals 0:

$$\sum_X i_X = 0, \quad \sum_X \frac{di_X}{dt} = 0, \quad \boldsymbol{T}^T \frac{d}{dt}\boldsymbol{i} = 0. \tag{9}$$

Multiplying Eq. 8 with the vector $\boldsymbol{T}^T$ and solving for the star point voltage v_S yields:

$$v_S = \frac{\boldsymbol{T}^T\boldsymbol{L}^{-1}\boldsymbol{v}_t - \boldsymbol{T}^T\boldsymbol{L}^{-1}\boldsymbol{R}\boldsymbol{i} + \boldsymbol{T}^T\frac{\boldsymbol{i}}{\boldsymbol{s}}\frac{d}{dt}\boldsymbol{s}}{\boldsymbol{T}^T\boldsymbol{L}^{-1}\boldsymbol{T}}. \tag{10}$$

By introducing the variables

$$\boldsymbol{L}_{\Sigma_X} = \boldsymbol{T}^T\boldsymbol{L}^{-1} = \left[L_{\Sigma_A}, L_{\Sigma_B}, L_{\Sigma_C}, L_{\Sigma_D}\right] \tag{11}$$

and (12)

$$\boldsymbol{L}_\Sigma = \boldsymbol{T}^T\boldsymbol{L}^{-1}\boldsymbol{T} = \boldsymbol{L}_{\Sigma X}\boldsymbol{T} \tag{13}$$

the previous expression can be simplified to the final expression for the star point voltage:

$$v_S = \frac{\boldsymbol{L}_{\Sigma_X}}{\boldsymbol{L}_\Sigma}\boldsymbol{v}_t - a(t) - b(t) \tag{14}$$

with

$$a(t) = \frac{\boldsymbol{L}_{\Sigma_i}}{\boldsymbol{L}_\Sigma}\boldsymbol{R}\boldsymbol{i}, \tag{15}$$

$$b(t) = \frac{\boldsymbol{T}^T}{\boldsymbol{L}_\Sigma}\frac{\boldsymbol{i}}{\boldsymbol{s}}\frac{d}{dt}\boldsymbol{s}. \tag{16}$$

2.2. Measurement procedure

In order to remove the common mode from the star point voltage, a measurement of the differential voltage $v_{SA} = v_S - v_A$ is used. Here, v_A is the voltage at the artificial star point, which is a resistor network, as illustrated in Fig. 1. Its voltage is given by:

$$v_A = \frac{1}{4}v_{DC}. \tag{17}$$

©2025 The Japan Society of Mechanical Engineers

In order to isolate the influence of a single coil on v_S and v_{SA}, the standard edge aligned PWM pattern has to be modified. The modified edge aligned PWM pattern is shown in Fig 2. The PWM pattern starts at t_0 where all inverter switches are open, thus the phase voltages are 0V. At t_1 one phase is connected to v_{DC} while the others phases remain not excited. The normal edge aligned PWM pattern continues at the time t_2. This pattern is permutated for every coil in the system. The presented approach allows a measurement of v_{SA} at the not excited state, at a time t_1^- immediately before t_1 and second measurement at the excited state t_1^+. At the time t_1^- the following states can be observed:

$$\boldsymbol{v}_t(t_1^-) = \mathbf{0}, \quad v_S(t_1^-) = -a(t_1^-) - b(t_1^-), \quad v_A(t_1^-) = 0, \quad v_{SA}(t_1^-) = v_S(t_1^-). \tag{18}$$

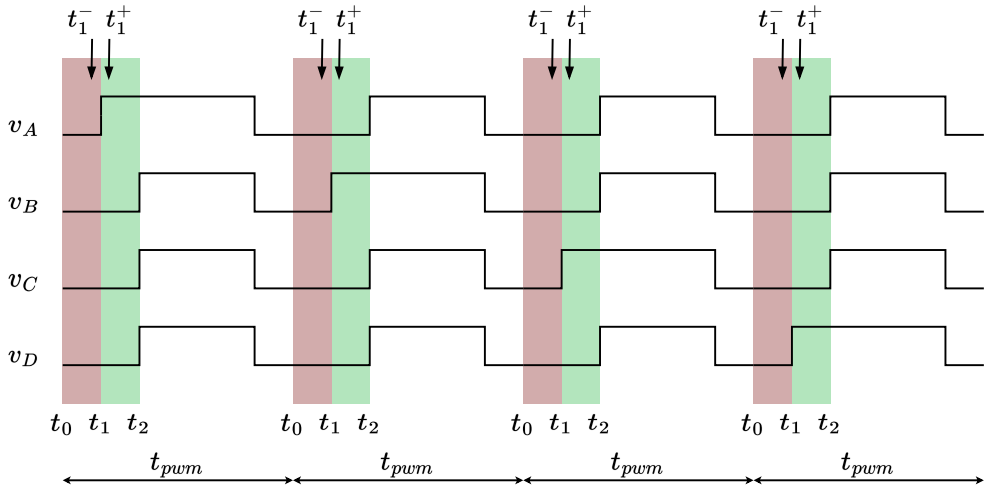

Fig. 2: Modified edge aligned PWM pattern repeated for each phase A-D.

At the excited state t_1^+ one can observe the following:

$$\boldsymbol{v}_t(t_1^+) = v_{DC}e_X, \quad v_S(t_1^+) = \frac{L_{\Sigma_i}}{L_\Sigma}\boldsymbol{v}_t - a(t_1^+) - b(t_1^+), \quad v_A(t_1^+) = \frac{1}{4}v_{DC}, \quad v_{SA}(t_1^+) = v_S(t_1^+) - v_A(t_1^+), \tag{19}$$

$$e_X = \begin{cases} [1,0,0,0]^T & \text{if } X = A \\ [0,1,0,0]^T & \text{if } X = B \\ [0,0,1,0]^T & \text{if } X = C \\ [0,0,0,1]^T & \text{if } X = D \end{cases} \tag{20}$$

with e_X being the unity vector as defined. It is now possible to compute the difference between both measurements

$$\Gamma_X = v_{SA}(t_1^+) - v_{SA}(t_1^-). \tag{21}$$

A typical value for t_1 is 10% of t_{pwm}. The actual value heavily depends on the system and oscillation of the star point voltage and can vary distinctly. However, t_1 still lies in the range of a few microseconds, concerning typical PWM frequencies in the kHz range. At these frequencies and fast measurements, it is possible to consider $a(t)$ and $b(t)$ as slow time constants and the term $\frac{L_{\Sigma_i}}{L_\Sigma}\boldsymbol{v}_t$ as a fast time constant of the system. It is therefore possible to define

$$a(t_1^-) = a(t_1^+), \qquad b(t_1^-) = b(t_1^+). \tag{22}$$

Now the expression for Γ can be written as

$$\Gamma_X = \left[\frac{\boldsymbol{L}_{\Sigma_X}}{\boldsymbol{L}_\Sigma} - \frac{1}{4}\right] v_{DC}e_X, \quad \boldsymbol{\Gamma} = \begin{bmatrix} \Gamma_A \\ \Gamma_B \\ \Gamma_C \\ \Gamma_D \end{bmatrix}. \tag{23}$$

©2025 The Japan Society of Mechanical Engineers

In the differential measurement of Γ the slow changing components $a(t)$ and $b(t)$ cancel each other out. The remaining expression for Γ is solely dependent on the ratio of all inductances in one phase and all inductances in the complete system and the DC supply voltage v_{DC}. If, as in this case, only self-inductances are taken into consideration and mutual-inductances are neglected, then $\boldsymbol{L}_{\Sigma_X} = L_X$. Thus Γ is the ratio of the self-inductance and the sum of all inductances scaled by v_{DC}.

2.3. Extracting the position information

Equation 4 shows, that the self-inductance of a single coil is solely depended on the air gap and other time invariant constants. Although, the neglected material coefficient μ_r can change with different operating conditions, such as the PWM frequency, or can go into saturation, it is assumed to stay constant during operation. With knowledge of μ_r under the given operating conditions, it is now possible to analytically reconstruct the position information from the measured values of Γ. However, this requires a comprehensive model of the material properties, which is often not available and requires effortful measurements and costly equipment. In addition, other effects like mutual inductances, eddy currents, hysteresis and fringing have been neglected, which leads to further inaccuracies in the analytic approach.

Another method to reconstruct the position information is the measurement of the Γ signals with a fixed rotor at different, known positions. This characterisation can be used in a lookup table or for curve-fitting to be implemented on a microcontroller. This method requires no further measurement equipment, besides the one used in operation anyway. However, an additional fixture for the rotor is needed. In the following chapter, the results of this characterisation are presented, followed by further experimental results.

3. Results

This section presents the experimental results of the previously proposed self-sensing method. Figure 3 shows a 3D model of the used plant as well as a close-up of one bearing with indication of the axis and phases. The here considered AMB is a four-phase, eight pole machine with heteropolar coil arrangement and a nominal air gap of 2mm. For reference, the actual position is measured with two laser position sensors at each bearing. The system and control strategy are described in detail in (Brasse et al., 2023; Vennemann et al., 2023).

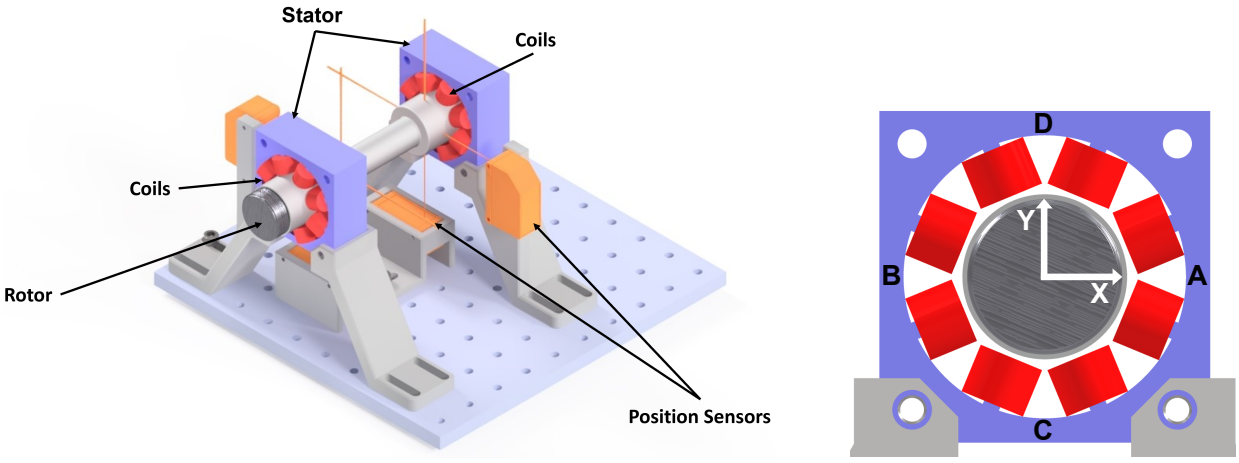

(a) (b)

Fig. 3: 3D overview over the plant used for experimental validation (a) and close-up of one bearing with indication of the axis and phases (b).

Figure 4 shows the measurements results of Γ for all four phases. Here, y and x denote the displacement of the rotor in x and y axis of the system. This characterisation is conducted with a mechanically fixed rotor and zero bias current at a PWM frequency of 20kHz. Thus, only a small measurement current of a few mA is present in the system. The characterisation is done at ± 1mm around the operating point. Further, the influence of the DC supply voltage v_{DC} has already been mathematically removed.

It is visible, that there is a variation of about 25% of the signals maximum as the rotor moves away from the

©2025 The Japan Society of Mechanical Engineers

respective coil. Changing the rotor position in the axis orthogonal to the coil, on the other hand, has very little effect on the signal. Further, the course of the signal around the operating point appears to be close to a linear behaviour. However, this assumption only holds true in the vicinity of the center position. If the edge areas of the air gap are included, the behaviour expected from Eq. 4 can be observed. Further, anisotropies can be noticed in the system, as the signal of the different phases is not identical and varies slightly at minimum and maximum values.

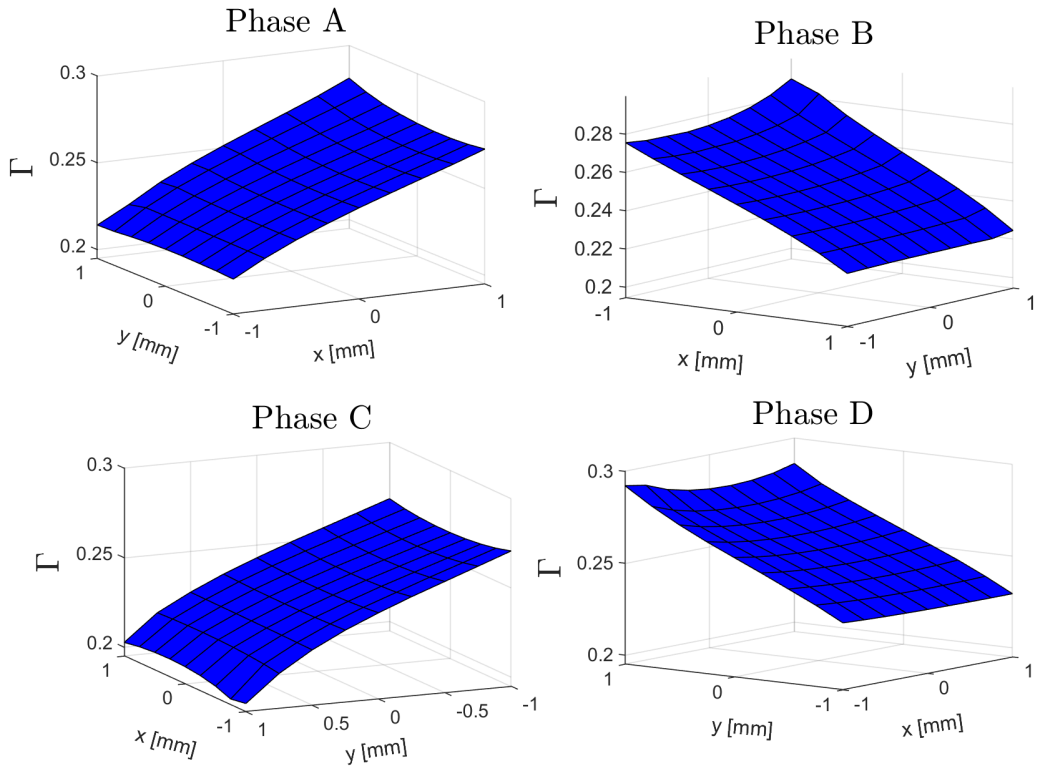

Fig. 4: Experimental measurement of Γ for all four phases at ± 1mm around the origin. Please note that x and y axis are swapped for enhanced readability in phases C and D.

In order to extract the position from the measured Γ signals, it is possible to define the differential signals

$$\Gamma_{AB} = \Gamma_A - \Gamma_B \tag{24}$$

and

$$\Gamma_{CD} = \Gamma_C - \Gamma_D. \tag{25}$$

Since the behaviour in Fig. 4 is almost linear, the following linear two dimensional polynomials are used to describe the position dependency in the Γ_{AB} and Γ_{CD} signals for each axis

$$x = 0.0651 + 0.0142 \cdot \Gamma_{AB} + 0.0019 \cdot \Gamma_{DC}, \tag{26}$$

$$y = 0.0722 + 0.0007 \cdot \Gamma_{AB} + 0.0155 \cdot \Gamma_{DC}. \tag{27}$$

The measurements of x and y, depending on Γ_{AB} and Γ_{CD} are shown in Fig. 5. The resulting planes are displayed alongside the measurements. It can be seen that the axis perpendicular to the coils has a major influence, while the other axis has only a minimal influence on the signals. The influence of the latter axis can be seen in the small tilt of the plane shown.

The generated polynomial fits are implemented on a microcontroller. In this experiment, only one bearing is operating, while the other is deactivated and in rest position to avoid coupling and tilting effects. The rotor does therefore not spin. The proposed self sensing algorithm is employed in the feedback loop, while the position sensors are just used for comparison. For position control, a second order sliding mode controller is used. Figure 6(a) shows the estimated and

©2025 The Japan Society of Mechanical Engineers

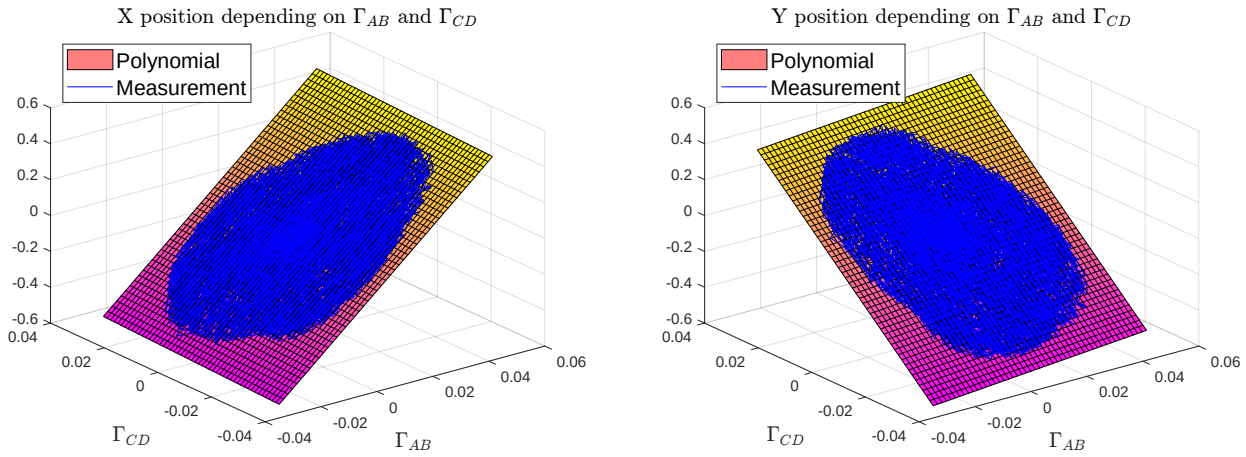

(a) (b)

Fig. 5: Polynomial fits for the reconstruction of x (a) and y (b) position along with measurements of the position, depending on the differential signals Γ_{AB} and Γ_{CD}.

measured position along with the circular reference position. The mean absolute estimation error in x and y direction amounts to 0.0008mm and -0.01mm, respectively. The higher error in the y axis can be explained with the gravity acting in this direction. Figure 6(b) shows the measured and estimated position as well, but with a constant reference position in the origin at $x = y = 0$. The estimation error in this configuration amounts to -0.003mm and 0.003mm, respectively. The estimation error is defined as the difference of the absolute estimated position and the absolute measured position and does therefore not include control errors.

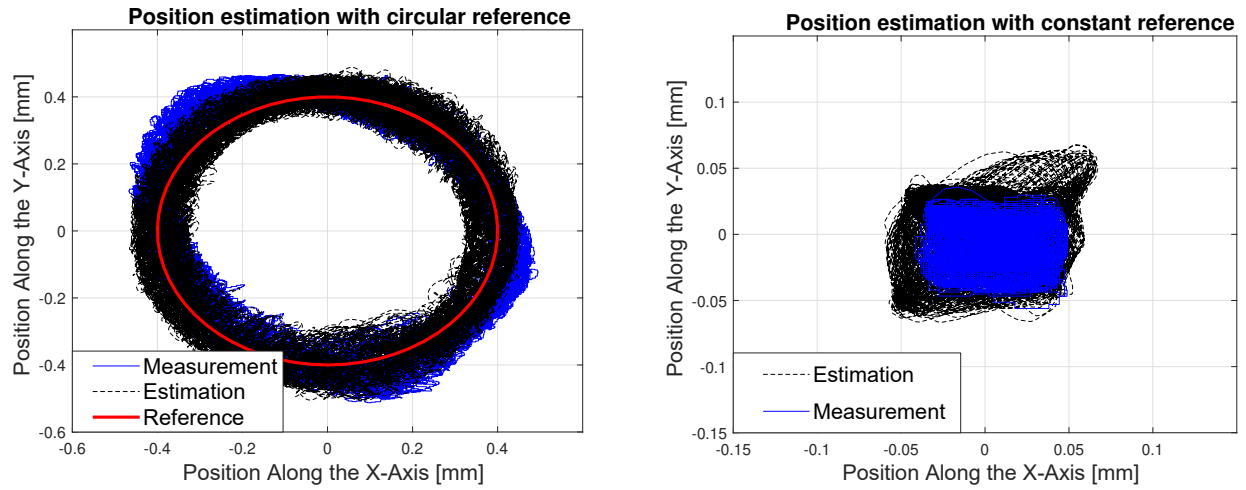

(a) (b)

Fig. 6: Measured and self-sensed position for a circular reference trajectory (a) and a constant reference (b) using the proposed method for position estimation in the feedback path of the control loop. Note the zoom for better visibility in Fig. (b).

4. Discussion and future work

The work analytically derives and experimentally validates a method for estimating the rotor position based on the star point voltage. It is shown, that the proposed measurements of the star point voltage theoretically only depend on the inductance of the coils and the DC supply voltage if the machine is not driven into saturation and effects like eddy currents are negligibly small. Further, mutual inductances have been neglected. The presented results show distinct position dependency on the measured signals. In experiments at zero rotor speed, with circular and constant reference

©2025 The Japan Society of Mechanical Engineers

positions, estimation errors from 0,8µm to 10µm can be observed. Thus, the star point voltage of an AMB actually carries useful information, that can be used for position estimation.

The usefulness of the proposed method compared to existing ones will be investigated in further studies. This research will also focus on the validation on a full scale bearing system with two radial and an axial bearing at non-zero rotor speed. This setup will be used to analyse the effects of rotor speed and current levels. Since the presented PWM pattern limits the controllers bandwidth and causes audible acoustic noise, alternative PWM patterns, as presented by (Schuhmacher, 2022), will be investigated.

Acknowledgments and Conflicts of Interest

Author Contributions: Conceptualization, J.V. and N.K.; methodology, J.V., N.K. and R.G.; Experimental Validation, R.G., N.K. and J.V.; formal analysis, J.V. and N.K.; Software, R.G., J.V. and N.K.; writing—original draft preparation, J.V.; writing—review and editing, N.K., M.N., R.G. and J.V.; funding acquisition, M.N and J.V.
Conflict of interest: The authors declare no conflict of interest.
Funding: The authors acknowledge funding from the Saarland ministry of finances and science within the call "Drittmittel.Transformation.Saarland".

References

Brasse, R., Vennemann, J., König, N., Nienhaus, M., and Grasso, E. (2023). Design and Implementation of a Driving Strategy for Star-Connected Active Magnetic Bearings with Application to Sensorless Driving. *Energies*, 16(1):396. Number: 1 Publisher: Multidisciplinary Digital Publishing Institute.

García, P., Guerrero, J. M., Briz, F., and Reigosa, D. D. (2010). Sensorless Control of Three-Pole Active Magnetic Bearings Using Saliency-Tracking-Based Methods. *IEEE Transactions on Industry Applications*, 46(4):1476–1484.

Grasso, E. (2021). *Direct Flux Control - a Sensorless Technique for Star-connected Synchronous Machines: An Analytic Approach*. Habilitation Thesis, Saarland University. Shaker Verlag.

Maslen, E. H. and Schweitzer, G., editors (2009). *Magnetic Bearings*. Springer Berlin Heidelberg, Berlin, Heidelberg.

Nenning, H. and Hutterer, S. (2014). Setup with Two Self-Sensing Magnetic Bearings Using Differential 3-Active INFORM. In *Proceedings of ISMB14*, Linz, Austria.

Niemann, A. and van Schoor, G. (2010). Self-Sensing Algorithm for Active Magnetic Bearings; Using Direct Current Measurements. In *Proceedings of ISMB12*, Wuhan, China.

Schuhmacher, K. (2022). *Position Estimation for PMSMs at Any Speed Using the Zero-Sequence Voltage and Modified Space Vector Modulation*. PhD thesis, Saarland University.

Thiemann, P., Mantala, C., Mueller, T., Strothmann, R., and Zhou, E. (2011). Direct Flux Control (DFC): A New Sensorless Control Method for PMSM. In *2011 46th International Universities' Power Engineering Conference (UPEC)*, pages 1–6.

Vennemann, J., Brasse, R., König, N., Nienhaus, M., and Grasso, E. (2023). Super Twisting Sliding Mode Control with Compensated Current Controller Dynamics on Active Magnetic Bearings with Large Air Gap. *Electronics*, 12(4):950. Number: 4 Publisher: Multidisciplinary Digital Publishing Institute.

©2025 The Japan Society of Mechanical Engineers